Activated Instability of Homogeneous Bubble Nucleation and Growth

Mark J. Uline and David S. Corti[*]

School of Chemcial Engineering, Purdue University, West Lafayette, Indiana 47907, USA
(Received 9 February 2007; published 16 August 2007)

For the superheated Lennard-Jones liquid, the free energy of forming a bubble with a given particle number and volume is calculated using density-functional theory. As conjectured, a consequence of known properties of the critical cavity [S. N. Punnathanam and D. S. Corti, J. Chem. Phys. **119**, 10 224 (2003)], the free energy surface terminates at a locus of instability. These stability limits reside, however, unexpectedly close to the saddle point. A new picture of homogeneous bubble nucleation and growth emerges from our study, being more appropriately described as an "activated instability."

Homogeneous bubble nucleation is the activated process by which the vapor phase is formed from a bulk super-heated liquid in the absence of impurities or solid surfaces [1]. According to classical nucleation theory (CNT) [1], if an embryo of the vapor phase is less than some critically sized bubble, the embryo collapses back into the super-heated liquid; if the embryo exceeds this critical size, the bubble grows to macroscopic size. Within CNT, the homogeneous nucleation rate is expressed in terms of the free energy, or reversible work, of forming embryos of various sizes. Since the vapor embryo is compressible, the free energy of formation is usually expressed as a function of the radius and internal pressure (or equivalently the number of particles n) of the (spherical) bubble [1,2]. The critical bubble then corresponds to the saddle point in free energy space: a maximum in the radius and a minimum in the internal pressure (or n). In addition, the free energy surface continues on indefinitely beyond the saddle point, serving to channel the embryo toward the lower lying minimum corresponding to the bulk vapor phase (e.g., Fig. 4 of Ref. [2]). Though this subsequent growth of nuclei may be rapid, the post-critical embryos nevertheless follow well-defined pathways that describe the reversible change of n and radii. In obtaining an expression for the nucleation rate, CNT also invokes another feature of the free energy surface, namely, that the region about the saddle point is sharply peaked [1]. Hence, only a small area centered about the saddle point describes the most likely transition paths between a precritical embryo and the vapor phase.

Recently, Punnathanam and Corti [3,4] focused on the relevance of cavities to bubble nucleation (a cavity is a spherical region devoid of particle centers), where density-functional theory (DFT) was employed to study cavity formation within the superheated Lennard-Jones (LJ) liquid [4]. For cavity radii less than some critical size, the superheated liquid was found to be stable (DFT yielded convergent liquidlike density profiles around the cavity). Beyond this critical cavity size, the superheated liquid became unstable (no convergent liquidlike density profile

was obtained). Molecular simulation verified the existence of the critical cavity [3]. A stability analysis revealed that the lowest eigenvalue of the matrix generated from the second-functional derivative of the grand potential went to zero at the critical cavity size [4], indicating that the critical cavity represents a true thermodynamic limit of stability. Also, the radius of the critical cavity λ_c was found to be a lower bound to the radius of the critical bubble, and the work of forming the critical cavity W_c was found to be a tight upper bound to the work of forming the critical bubble W_b [4]. These results suggest that cavities play an important role in the process of bubble nucleation, a conclusion that is not inconsistent with the apparent dominant role that cavities play in the initial stages of phase transitions in liquids as seen in previous molecular simulation studies [5].

Specifically, the existence of a critical cavity necessarily implies that the free energy surface $W(n, v)$ of bubble formation, where n is the number of particles inside a bubble of volume v, is very different from what follows from CNT [2]. The critical cavity, or terminus of the $n = 0$ profile, should be in a sense "felt" throughout $W(n, v)$. In other words, we suspect that a limit of stability will be reached for each n, with the radius of the bubble at this stability limit increasing with an increase in n. For small n, W at the limit of stability should decrease with an increase in n (because $W_c > W_b$). Along $n = n^*$, where n^* is the number of particles inside the critical bubble, a maximum of W with respect to v will appear before the stability limit is reached, since the critical bubble corresponds to a saddle point. For some n in between $n = 0$ (where no maximum appears [3]) and $n = n^*$, other maxima should also develop before limits of stability are reached. Since the stability limits near the saddle point are located after maxima (beyond the barrier), they may be irrelevant to the early stages of bubble nucleation.

This conjectured view of the free energy surface is different from previous constructions of the bubble surface and offers a new and intriguing picture of the molecular mechanism of bubble nucleation. For one, a *locus of instability* appears, describing the values of n and v at which

the free energy surface terminates; $W(n, v)$ no longer continues on indefinitely toward the vapor phase. The growth of bubbles beyond this locus of instability should follow, by definition, a mechanism appropriate for unstable fluids. Consequently, bubble nucleation and growth is better described as an "activated instability": embryos surmount a free energy barrier only to initiate an instability. Interesting effects may arise if the stability limits run near to the saddle point. Since W_c is a tight upper bound to W_b, and no maximum appears for $n = 0$, embryos may likely follow trajectories that bypass the saddle and reach a limit of stability without having traversed a maximum.

To test the above conjecture, at least for the pure component LJ liquid (with the potential truncated and shifted at 4σ [4], where σ is the LJ diameter), we construct $W(n, v)$ via DFT, modified to obtain the separate density profiles that develop inside and outside a given volume v, with the number of particles n inside v held fixed. The bubble density profile is labeled as $\rho_{\text{in}}(\vec{r}_1)$, while the density profile of the liquid surrounding the bubble is $\rho_{\text{out}}(\vec{r}_2)$. With a spherical bubble of radius λ centered at the origin, $\vec{r}_1$ is defined for $0 \leq |\vec{r}_1| \leq \lambda$ and $\vec{r}_2$ is defined for $|\vec{r}_2| \geq \lambda$. The constraint of fixed particle number, $n = \int \rho_{\text{in}}(\vec{r}_1)d\vec{r}_1$, is imposed using a Lagrange mulitplier κ [6]. Invoking the local density and random phase approximations [7], the grand potential Ω of the system is given by

$$\Omega = \int f_h[\rho_{\text{in}}(\vec{r}_1)]d\vec{r}_1 + \frac{1}{2} \iint \rho_{\text{in}}(\vec{r}_1)\rho_{\text{in}}(\vec{r}_1')\phi_2(\vec{r}_1, \vec{r}_1')d\vec{r}_1 d\vec{r}_1' + \int f_h[\rho_{\text{out}}(\vec{r}_2)]d\vec{r}_2$$
$$+ \frac{1}{2} \iint \rho_{\text{out}}(\vec{r}_2)\rho_{\text{out}}(\vec{r}_2')\phi_2(\vec{r}_2, \vec{r}_2')d\vec{r}_2 d\vec{r}_2' - \mu \int \rho_{\text{out}}(\vec{r}_2)d\vec{r}_2 + \iint \rho_{\text{in}}(\vec{r}_1)\rho_{\text{out}}(\vec{r}_2)\phi_2(\vec{r}_1, \vec{r}_2)d\vec{r}_1 d\vec{r}_2$$
$$- \kappa\Big(n - \int \rho_{\text{in}}(\vec{r}_1)d\vec{r}_1\Big) - n\mu. \tag{1}$$

f_h is the Helmholtz free energy density of the reference hard sphere fluid and ϕ_2 is the attractive part of the LJ potential via Weeks, Chandler, and Anderson [8]. Since n is fixed, the chemical potential μ of the bulk liquid is only imposed on the region exterior to the bubble. The reversible work of removing n particles from the bulk liquid is equal to $n\mu$ [9] and ensures that the work of bubble formation, $W(n, v) = \Omega - \Omega_0$, is accounted for properly, where Ω_0 is the grand potential of the uniform liquid. The equilibrium density profiles are found from the two functional derivatives of Eq. (1) with respect to ρ_{in} and ρ_{out}, respectively, which when each is set to zero yield

$$\mu = \mu_h[\rho_{\text{out}}(\vec{r}_2)] + \int \rho_{\text{in}}(\vec{r}_1)\phi_2(\vec{r}_1, \vec{r}_2)d\vec{r}_1 + \int \rho_{\text{out}}(\vec{r}_2')\phi_2(\vec{r}_2, \vec{r}_2')d\vec{r}_2'$$
$$\kappa = \mu_h[\rho_{\text{in}}(\vec{r}_1)] + \int \rho_{\text{in}}(\vec{r}_1')\phi_2(\vec{r}_1, \vec{r}_1')d\vec{r}_1' + \int \rho_{\text{out}}(\vec{r}_2)\phi_2(\vec{r}_1, \vec{r}_2)d\vec{r}_2 \tag{2}$$
$$n\exp(-\kappa/kT) = \frac{1}{\Lambda^3} \int \exp\Big[-\frac{\mu_h^{\text{ex}}[\rho_{\text{in}}(\vec{r}_1')]}{kT} - \frac{1}{kT} \int \rho_{\text{in}}(\vec{r}_1'')\phi_2(\vec{r}_1', \vec{r}_1'')d\vec{r}_1'' - \frac{1}{kT} \int \rho_{\text{out}}(\vec{r}_2)\phi_2(\vec{r}_1', \vec{r}_2)d\vec{r}_2 \Big]d\vec{r}_1',$$

where k is Boltzmann's constant, Λ is the de Broglie wavelength, and μ_h^{ex} is the excess chemical potential of the hard sphere fluid (whose diameter is chosen as in Ref. [4]).

A plot of $W(n, v)$ versus λ for different values of n at a temperature of $kT/\epsilon = 0.8$ (ϵ is the LJ well depth) and a bulk density of $\rho_b\sigma^3 = 0.8$ is provided in Fig. 1. As anticipated, each n profile terminates at a limit of stability, λ_{sl} (for $\lambda > \lambda_{\text{sl}}$, ρ_{out} did not converge to a liquidlike density profile), with λ_{sl} increasing with an increase in n. λ_{sl} was also shown to coincide with the vanishing of the lowest eigenvalue of the matrix generated from the second-functional derivative of Ω with respect to ρ_{out}, verifying that each λ_{sl} corresponds to a true thermodynamic limit of stability. (Since n is fixed and the surrounding liquid does not impose its chemical potential on the bubble, only the stability of the surrounding metastable liquid need be considered; i.e., only the curvature of Ω with respect to

variations in ρ_{out} is evaluated.) Furthermore, as n increases, maxima develop in the work profiles (the minima correspond to bubble densities for which $n/v \approx \rho_b$). Surprisingly, limits of stability appear just beyond these maxima. In Fig. 1, the saddle point is located at $n^* \approx 10$ and $\lambda \approx 3.78\sigma$, corresponding to $W_b/\epsilon \approx 68.66$. Using the standard DFT approach [7], which is based on a single density profile and can only locate the saddle point, the work of forming the critical bubble is $W_b/\epsilon = 68.66$. In Fig. 2, the density profile of the critical bubble obtained from standard DFT is compared with ρ_{in} and ρ_{out} at the saddle point in Fig. 1. Taken together, ρ_{in} and ρ_{out} yield a density profile that is nearly indistinguishable from the previous result, suggesting that our modified DFT relations generate a physically meaningful free energy surface consistent with other studies of bubble nucleation.

Two striking, and newly predicted, features of Fig. 1 as compared with CNT [2] are (1) the appearance of a *locus of*
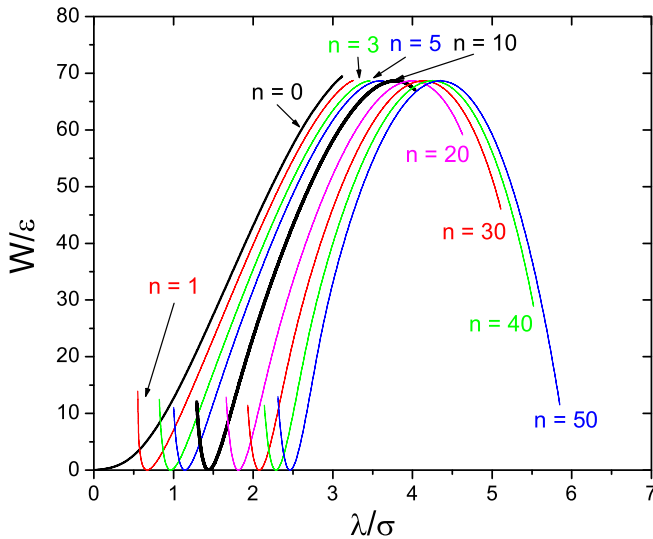
FIG. 1 (color online).   The reversible work W of forming a bubble with a given particle number n and radius λ within the superheated LJ liquid at $kT/\varepsilon = 0.8$ and $\rho_b\sigma^3 = 0.7$ ($\rho_b\sigma^3$ at the spinodal and binodal are 0.647 and 0.855, respectively). The saddle point is located at $n \approx 10$, $\lambda/\sigma \approx 3.78$, and $W_b/\varepsilon \approx 68.66$.

instability and (2) the proximity of this locus to the saddle point (stability limits appear *just* beyond the saddle point). In addition, W_c ($= 69.47\epsilon$) slightly exceeds W_b ($= 68.66\epsilon$). All of these aspects of the free energy surface are clearly seen in the three-dimensional view provided in Fig. 3, where beyond the locus of instability no stable representation of $W(n, \upsilon)$ exists. Figures 1 and 3 suggest that bubble nucleation and growth is more aptly described as an "activated instability." An embryo must still over-
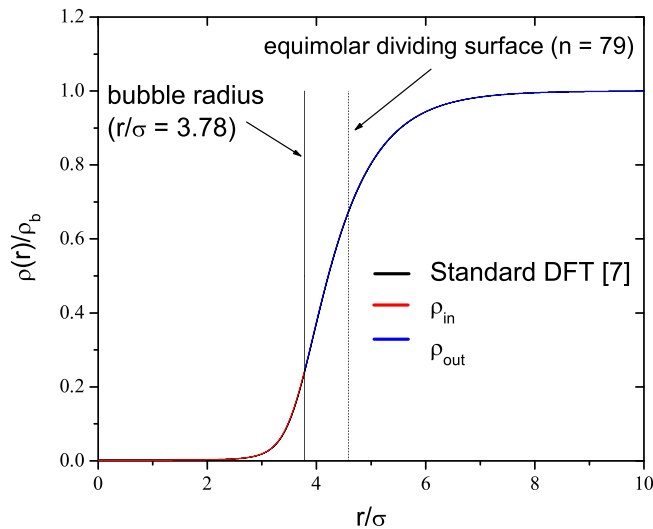

FIG. 2 (color online).   The bubble and surrounding liquid density profiles, relative to the bulk density ρ_b, for the saddle point in Fig. 1.
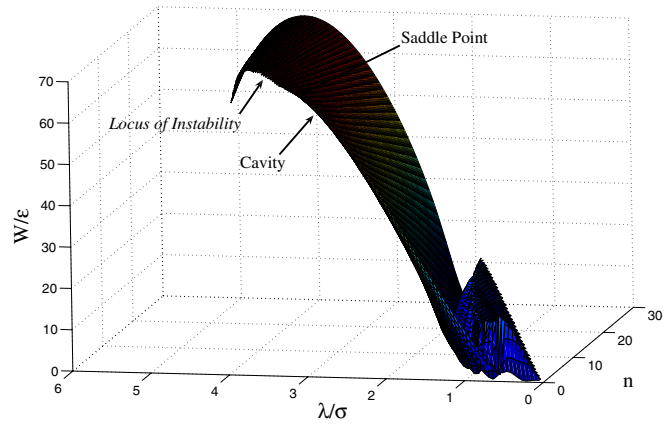

FIG. 3 (color online).   Three-dimensional view of $W(n/\upsilon)$ given in Fig. 1.

come a free energy barrier before reaching the locus of instability, where it causes the metastable liquid to become unstable. Further growth of the embryo is spontaneous, not because the free energy surface rapidly channels the bubble toward the much lower lying free energy minimum (the bulk vapor), but given that growth beyond the stability limit proceeds via a mechanism appropriate for phase separations in unstable systems. Since W_c exceeds W_b by only 1.01 kT, Fig. 3 also suggests that embryos will reach a limit of stability not only by traversing the free energy barrier at the saddle point, but by following trajectories that
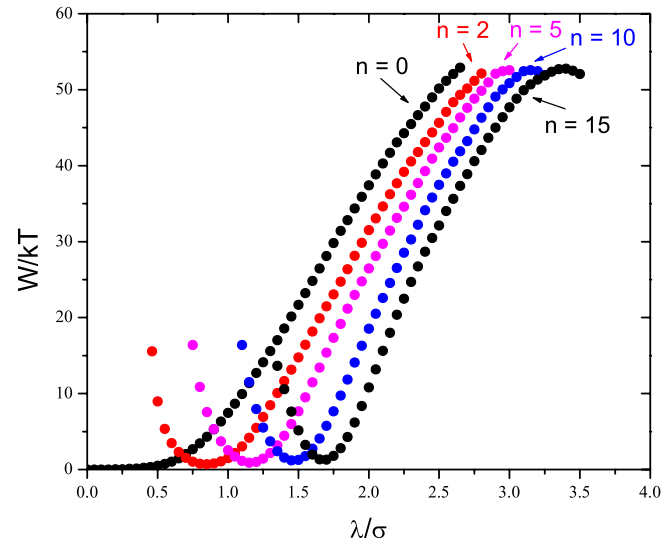

FIG. 4 (color online).   The reversible work W of forming a bubble within the superheated LJ liquid at $kT/\epsilon = 0.8$ and $P\sigma^3/\varepsilon = -0.329$ obtained from isothermal-isobaric Monte Carlo simulations (at the spinodal and binodal, $P\sigma^3/\varepsilon$ are $\simeq -0.600$ and $\simeq 0.006\,17$, respectively [11]). W at the limits of stability for $n = 0$ and $n = 2$ (which do not exhibit maxima) are $\sim$52.9 and $\sim$52.1 kT, respectively, while at the maxima for $n = 5$, $n = 10$, and $n = 15$, $W \sim 52.6$, $\sim$52.7, and $\sim$52.8 kT, respectively. The saddle point resides around $n = 5$.

terminate at the locus of instability for $n < n^*$ (barrier crossings away from the saddle have been considered before [10]). Cavities, as well as small particle bubbles, may therefore play an important role in the initial stages of the liquid-to-vapor transition, a conclusion not inconsistent with the simulation studies of bubble nucleation performed in Refs. [5]. A similar result holds for $n > n^*$ where, for example, the maximum value of W for $n = 30$ is only ≈ 0.04 kT greater than W_b.

To verify the key aspects of Figs. 1 and 3, we performed isothermal-isobaric Monte Carlo simulations to calculate $W(n, v)$ for the same LJ superheated liquid at $kT/\epsilon = 0.8$ and a pressure of $P\sigma^3/\epsilon = -0.329$ (the average bulk density is $\rho_b\sigma^3 = 0.735$; work profiles were constructed using the method described in Ref. [3]). The simulation results shown in Fig. 4 confirm that a stability limit is reached for each n, whereby the liquid density far from the bubble surface could not be maintained at its bulk value upon a further increase in the radius [3]. In addition, the limits of stability for $n = 5$ and $n = 10$ appear just beyond each maxima of W. The saddle point appears to reside around $n = 5$, which is consistent with the DFT predictions.

In conclusion, a new picture of homogeneous bubble nucleation and growth emerges from our DFT and simulation studies. In particular, a locus of instability appears on the free energy surface for bubble formation, suggesting that nucleation and growth is more appropriately viewed as an "activated instability." One suspects that limits of stability will arise at other superheated liquid state points (beyond the one condition studied here). Whether these loci of instability also reside close to the saddle point remains to be seen. Although the emerging view of the molecular-level details of nucleation and growth are quite different from what was previously thought, one may wonder why such differences have not been noted already. For one, the overall picture, or the net effect of bubble nucleation (at least as seen from a coarse-grained or mesoscopic scale), has not drastically changed. Vapor embryos still "see" a free energy barrier that must be surmounted. Hence, the limits of stability should be irrelevant to the early stages of nucleation, when the initial distribution of embryos is just forming, and a nucleation rate should still be expressible in terms of a barrier height. Once a stability limit is reached, the growth of the bubble should proceed quite rapidly, although now via some mechanism suitable for an unstable fluid. The prediction of an unstable growth phase is intriguing and certainly unexpected. (This detail of the process is clearly what differs from the previous description of bubble nucleation and growth, and future work is directed towards identifying a corresponding signature

of such an unstable growth phase.) Yet, we note that the bubble should trigger a "local instability" as opposed to the "global instability" that develops upon entering the spinodal region, where phase separation occurs by spinodal decomposition [1]. Within the spinodal region, the entire uniform liquid is unstable. In contrast, the instability generated by the bubble is a consequence of an inhomogeneity that propagates only a finite distance within the liquid. Thus, far from the bubble another uniform portion of the liquid, which is metastable and so thermodynamically stable, should be unaware of the instability just initiated. Upon reaching a stability limit the bubble creates a local instability, spontaneously growing thereafter, but without affecting the intrinsic stability of other regions of the superheated liquid. Consequently, many widely separated bubbles can grow to macroscopic size and eventually coalesce, a scenario not different from what is already seen to occur. Of course, additional investigations are needed to verify the growth of bubbles due to local instabilities, elucidate further the molecular-based mechanisms by which this stage of the liquid-to-vapor transition transpires, as well as determine quantitatively how the kinetics of bubble nucleation and growth should differ when modeled as an activated instability.

*dscorti@ecn.purdue.edu

[1] P. G. Debenedetti, *Metastable Liquids* (Princeton University Press, Princeton, NJ, 1996).

[2] L. Gunther, Am. J. Phys. **71**, 351 (2003).

[3] S. N. Punnathanam and D. S. Corti, Ind. Eng. Chem. Res. **41**, 1113 (2002).

[4] S. N. Punnathanam and D. S. Corti, J. Chem. Phys. **119**, 10 224 (2003).

[5] T. Kinjo and M. Matsumoto, Fluid Phase Equilib. **144**, 343 (1998); V. K. Shen and P. G. Debenedetti, J. Chem. Phys. **111**, 3581 (1999); D. Zahn, Phys. Rev. Lett. **93**, 227801 (2004).

[6] V. Talanquer and D. W. Oxtoby, J. Chem. Phys. **100**, 5190 (1994).

[7] X. C. Zeng and D. W. Oxtoby, J. Chem. Phys. **94**, 4472 (1991).

[8] J. D. Weeks, D. Chandler, and H. C. Anderson, J. Chem. Phys. **54**, 5237 (1971).

[9] B. Senger *et al.*, J. Chem. Phys. **110**, 6421 (1999).

[10] B. E. Wyslouzil and G. Wilemski, J. Chem. Phys. **103**, 1137 (1995); J. W. P. Schmelzer, G. S. Boltachev, and V. G. Baidakov, J. Chem. Phys. **124**, 194503 (2006).

[11] J. K. Johnson, J. A. Zollweg, and K. E. Gubbins, Mol. Phys. **78**, 591 (1993).